Basic Res Cardiol (2012) 107:236
DOI 10.1007/s00395-011-0236-2

ORIGINAL CONTRIBUTION

Sgk1 sensitivity of Na^+/H^+ exchanger activity and cardiac remodeling following pressure overload

Jakob Voelkl · Yun Lin · Ioana Alesutan · Mohamed Siyabeldin E. Ahmed · Venkanna Pasham · Sobuj Mia · Shuchen Gu · Martina Feger · Ambrish Saxena · Bernhard Metzler · Dietmar Kuhl · Bernd J. Pichler · Florian Lang

Received: 19 August 2011 / Revised: 15 November 2011 / Accepted: 4 December 2011 / Published online: 3 January 2012

Abstract Sustained increase of cardiac workload is known to trigger cardiac remodeling with eventual development of cardiac failure. Compelling evidence points to a critical role of enhanced cardiac Na^+/H^+ exchanger (NHE1) activity in the underlying pathophysiology. The signaling triggering up-regulation of NHE1 remained, however, ill defined. The present study explored the involvement of the serum- and glucocorticoid-inducible kinase Sgk1 in cardiac remodeling due to transverse aortic constriction (TAC). To this end, experiments were performed in gene targeted mice lacking functional Sgk1 ($sgk1^{-/-}$) and their wild-type controls ($sgk1^{+/+}$). Transcript levels have been determined by RT-PCR, cytosolic pH (pH_i) utilizing 2′,7′-bis-(2-carboxyethyl)-5-(and-6)-carboxyfluorescein (BCECF) fluorescence, Na^+/H^+ exchanger activity by the Na^+-dependent realkalinization after an ammonium pulse, ejection fraction (%) utilizing cardiac cine magnetic resonance imaging and cardiac glucose uptake by PET imaging. As a result, TAC increased the mRNA expression of Sgk1 in $sgk1^{+/+}$ mice, paralleled by an increase in Nhe1 transcript levels as well as Na^+/H^+ exchanger activity, all effects virtually abrogated in $sgk1^{-/-}$ mice. In $sgk1^{+/+}$ mice, TAC induced a decrease in Pgc1a mRNA expression, while Spp1 mRNA expression was increased, both effects diminished in the $sgk1^{-/-}$ mice. TAC was followed by a significant increase of heart and lung weight in $sgk1^{+/+}$ mice, an effect significantly blunted in $sgk1^{-/-}$ mice. TAC increased the transcript levels of Anp and Bnp, effects again significantly blunted in $sgk1^{-/-}$ mice. TAC increased transcript levels of Collagen I and III as well as Ctgf mRNA and CTGF protein abundance, effects significantly blunted in $sgk1^{-/-}$ mice. TAC further decreased the ejection fraction in $sgk1^{+/+}$ mice, an effect again attenuated in $sgk1^{-/-}$ mice. Also, cardiac FDG-glucose uptake was increased to a larger extent in $sgk1^{+/+}$ mice than in $sgk1^{-/-}$ mice after TAC. These observations point to an important role for SGK1 in cardiac remodeling and development of heart failure following an excessive work load.

Keywords Nhe1 · Na^+/H^+ exchanger · PI3 kinase · Sgk1 · Heart failure

Abbreviations

Anp	Atrial natriuretic peptide
Bnp	Brain natriuretic peptide
Ctgf	Connective tissue growth factor
EF	Ejection fraction [(end-diastolic volume – end-systolic volume)/end-diastolic volume]
LV	Left ventricle
MRI	Magnetic resonance imaging
NHE	Na^+/H^+ exchanger

Electronic supplementary material The online version of this article (doi:10.1007/s00395-011-0236-2) contains supplementary material, which is available to authorized users.

J. Voelkl · I. Alesutan · M. S. E. Ahmed · V. Pasham · S. Mia · S. Gu · M. Feger · A. Saxena · F. Lang (✉)
Department of Physiology, University of Tübingen, Gmelinstr. 5, 72076 Tübingen, Germany
e-mail: florian.lang@uni-tuebingen.de

J. Voelkl · B. Metzler
Department of Cardiology, Medical University Innsbruck, Anichstr 35, 6020 Innsbruck, Austria

Y. Lin · B. J. Pichler
Laboratory for Preclinical Imaging and Imaging Technology of the Werner Siemens-Foundation, Department of Preclinical Imaging and Radiopharmacy, University of Tübingen, Roentgenweg 13, 72076 Tübingen, Germany

D. Kuhl
University Medical Center Hamburg-Eppendorf (UKE), Falkenried 94, 20251 Hamburg, Germany

Pgc1a	Peroxisome proliferator activated receptor γ coactivator 1 alpha
PI3K	Phosphatidylinositide 3 kinase
PET	Positron emission tomography
SGK1	Serum- and glucocorticoid-inducible kinase 1
TAC	Transverse aortic constriction

Introduction

Chronically increased cardiac workload may lead to cardiac remodeling with eventual cardiac failure [29, 77]. Typical features of cardiac remodeling include an altered metabolic phenotype consisting of reduced cardiac fatty acid oxidation, increased glycolysis and increased glucose oxidation [52, 62]. The cardiac remodeling is further paralleled by enhanced NADPH oxidase activity [68].

The cardiac hypertrophy and heart failure following chronic stimulation of the β_1-adrenergic receptor [13, 25] is reversed by inhibition of the Na^+/H^+ exchanger NHE1 by cariporide [25]. Similarly, NHE1 is critically important for postinfarction remodeling [41–46, 48] and estrogen-induced ventricular cardiac hypertrophy [49]. Along these lines, cardiac hypertrophy and heart failure can be triggered by overexpression of NHE1 [70]. Accordingly, NHE1 inhibition has been considered a therapeutic option in the treatment of heart failure [11, 48, 64].

NHE1 plays a pivotal role in the regulation of cytosolic pH [73, 76], which is in turn decisive for the flux through glycolysis and thus glucose utilization [15]. Glycolysis is stimulated by cytosolic alkalinization and disrupted by cytosolic acidification [15]. NHE1 activity further governs cell volume [40, 55]. Increased NHE activity leads to cell swelling, which is in turn a powerful stimulator of protein synthesis and inhibitor of proteolysis, both effects favoring cellular hypertrophy [39, 55]. Moreover, NHE1 activity is critically important for NADPase activity and thus formation of reactive oxygen species [19, 32].

Mechanisms accounting for the up-regulation of NHE1 activity in the failing heart are incompletely understood. Several models of cardiac hypertrophy involve signaling through phosphatidylinositide 3 kinase PI3K [9, 20, 36, 37, 74, 82, 102] which in turn participates in the regulation of NHE activity [51, 86, 87, 91].

The serum- and glucocorticoid-inducible kinase SGK1 [54, 56], a kinase genomically regulated by glucocorticoids [27], mineralocorticoids [18, 71, 89], 1,25-dyhydroxyvitamin D_3 [1,25$(OH)_2D_3$] [2], cell shrinkage [95], gonadotropins [7, 8, 35, 79], and TGFβ [58, 96], is stimulated by PI3K through phosphoinositide-dependent kinase PDK1 [3, 4, 21, 31, 50, 53, 75]. SGK1 expression is particularly abundant in fibrosing tissue [26, 58, 92, 96]. Activation and expression of SGK1 has been shown to be stimulated by pressure overload [10].

SGK1 has previously been shown to regulate a wide variety of carriers [5, 14, 33, 54, 56, 78] including the epithelial Na^+/H^+ exchanger NHE3 [30, 97, 103]. Also, SGK1 has previously been shown to be required for induction of cardiac fibrosis by mineralocorticoid excess [92].

The present study has thus been performed to elucidate whether SGK1 participates in cardiac remodeling following increased workload. To this end, the impact of transverse aortic constriction on cardiac Nhe1 and cardiac hypertrophy [81] was evaluated in gene targeted mice lacking functional Sgk1 ($sgk1^{-/-}$) and their wild-type controls ($sgk1^{+/+}$).

Materials and methods

Animals

All animal experiments were conducted according to the German law for the welfare of animals and were approved by local authorities. As described previously [99], a conditional targeting vector was generated from a 7-kb fragment encompassing the entire transcribed region on 12 exons. The neomycin resistance cassette was flanked by two loxP sites and inserted into intron 11. Exons 4–11, which code for the *sgk1* domain, were "floxed" by inserting a third loxP site into intron 3. Targeted R1 ES cells were transiently transfected with Cre recombinase. A clone with a recombination between the first and third loxP site (type I recombination) was injected into C57BL/6 blastocytes. Male chimeras were bred to 129/SvJ females. Heterozygous *sgk1*-deficient mice were backcrossed to 129/SvJ wild-type mice for two generations and then intercrossed to generate homozygous $sgk1^{-/-}$ and $sgk1^{+/+}$ littermates. The animals were genotyped by PCR using standard methods. The study has been performed in 8- to 10-week-old matched female and male $sgk1^{+/+}$ and $sgk1^{-/-}$ mice. Prior to the experiments, mice had free access to control diet and tap drinking water.

Aortic banding

Cardiac pressure overload was induced in 8- to 10-week-old mice as described [81]. Briefly, mice were anesthetized by a mixture of midazolam (5 mg/kg b.w.), medetomidine (0.5 mg/kg b.w.) and fentanyl (0.05 mg/kg b.w.) and placed on a heating pad. After intubation and ventilation (Harvard minivent, Harvard apparatus, Holliston, USA), the second intercostal space was opened by a small incision. The transverse aorta was exposed and constricted

between the truncus brachiocephalicus and the left carotid artery by the width of a 27-G canula using a 7-0 nylon suture. Sham treatment was performed similarly but without constriction of the filament. After closing the access site, anesthesia was antagonized by injection of atipamezol (2.5 mg/kg b.w.) and flumazenil (0.5 mg/kg b.w.) and animals were monitored until recovery. Animals were treated with buprenorphine (0.05 mg/kg b.w.) for 2 days after procedure. In one study group, before sacrificing, the right common carotid artery was catheterized with a pressure catheter (WPI FO BPS, World precision instruments, Sarasota, USA) to evaluate blood pressure 1 week after the procedure. Animals were sacrificed 1 week or 5 weeks after the procedure.

MRI imaging

MRI scans were performed on a 7T small animal MR system (ClinScan; Bruker BioSpin GmbH, Ettlingen, Germany) using a 35-mm mouse whole body coil (Bruker). Mice were anesthetized by 1.2–1.5% isoflurane evaporated in 100% medical oxygen and placed in prone position on a customized animal bed connected to feedback heating controller with a rectal temperature probe. The heart and respiratory rates were monitored by placing ECG electrodes subcutaneously into the paw and a respiratory pillow under the torso (SA Instruments, Stony Brook, NY, USA). MRI scans were ECG triggered and respiratory gated. The mouse hearts were localized by a scout scan. The short axial view in multiple planes covering the entire heart and the long axial view in one plane perpendicular to the short axial view were acquired in cine mode (flip angle, 25°; matrix size, 384 × 384; voxel size, 0.091 × 0.091 × 1 mm; number of averaged images, 2–4, 15–25 frames/cardiac cycle). MRI images were analyzed in image J software (http://rsbweb.nih.gov/ij/). End-systole was defined as the maximum contraction of the heart during the cardiac cycle; end-diastole was defined as the maximum relaxation of the heart during the cardiac cycle. Ejection fraction was calculated from short axis images covering the whole ventricle using the standard formula ([end-diastolic volume – end-systolic volume]/end-diastolic volume) [93].

PET imaging

PET measurement took place at separate nonconsecutive days of MRI study. The mice were anesthetized by inhalation of 1.2–1.5% isoflurane evaporated in 0.8 L/min oxygen using a dedicated rodent anesthesia system (Vetland, KT, USA). All mice were fasted 11–17 h before injection of 12.86 ± 0.69 MBq [^{18}F]FDG tracer [38] via the tail vein. After a 55 min tracer uptake period in an anesthesia box, the mice were transferred to a small animal PET scanner (Inveon; Siemens Healthcare, Knoxville, TN, USA) with the hearts centered in the field of view (FOV). PET emission data were acquired for 15 min followed by a 13-min transmission scan for photon attenuation correction. During the PET scans mice were maintained at constant body temperature. The PET scanner yields a spatial resolution of about 1.4 mm in the reconstructed images. The PET images were reconstructed into 128 × 128 matrix (voxel size, 0.776 × 0.776 × 0.796 mm) by an ordered subset expectation maximization (OSEM) 2D-algorithm applying attenuation correction using the Inveon Acquisition Workplace (v1.4.3.6 and v1.5.0.28) software. Regions of interests (ROIs) were placed in six consecutive slices of the left myocardium in short axial view, and the counts of left ventricle cavity were subtracted. The myocardial [^{18}F]FDG uptake was calculated as standardized uptake value (SUV).

Quantitative RT-PCR

After killing the animals, cardiac tissue was immediately snap frozen in liquid nitrogen. Total RNA was isolated from mouse heart by using Trifast Reagent (Peqlab, Erlangen, Germany) according to the manufacturer's instructions. Reverse transcription of 2 μg RNA was performed using oligo(dT)$_{12–18}$ primers (Invitrogen, Karlsruhe, Germany) and SuperScript III Reverse Transcriptase (Invitrogen, Karlsruhe, Germany). cDNA samples were treated with RNase H (Invitrogen, Karlsruhe, Germany). Quantitative real-time PCR was performed with the iCycler iQ™ Real-Time PCR Detection System (Bio-Rad Laboratories, Hercules, CA) and iQ™ Sybr Green Supermix (Bio-Rad Laboratories, Hercules, CA) according to the manufacturer's instructions. The following primers were used (5′ → 3′ orientation):

NheI fw: GCCATTGAGCTGGTGGAGAG;
NheI rev: CGGTCTGAAGTCACAGCCTTG;
Sgk1 fw: CTGCTCGAAGCACCCTTACC;
Sgk1 rev: TCCTGAGGATGGGACATTTTCA;
Gapdh fw: AGGTCGGTGTGAACGGATTTG;
Gapdh rev: TGTAGACCATGTAGTTGAGGTCA;
Col1a1 fw: ACCCGAGGTATGCTTGATCTG;
Col1a1 rev: CATTGCACGTCATCGCACAC;
Col3a1 fw: CCATTTGGAGAATGTTGTGCAAT;
Col3a1 rev: GGACATGATTCACAGATTCCAGG;
Ctgf fw: GACCCAACTATGATGCGAGCC;
Ctgf rev: TCCCACAGGTCTTAGAACAGG;
Pgc-1α fw: AGACGGATTGCCCTCATTTGA;
Pgc-1α rev: TGTAGCTGAGCTGAGTGTTGG;
Spp1 fw: GACCATGAGATTGGCAGTGA;
Spp1 rev: GGAACTGTGTTTTTGCCTCTT.

The specificity of the PCR products was confirmed by analysis of the melting curves and in addition by agarose gel electrophoresis.

To determine Anp (Nppa) and Bnp (Nppb) transcript levels, quantitative real-time PCR was performed with the iCycler iQ^{TM} Real-Time PCR Detection System (Bio-Rad Laboratories, Hercules, CA) using Universal TaqMan Master Mix (Applied Biosystems, Foster City, CA, USA) as recommended by the manufacturer. TaqMan primers and probes for Nppa, Nppb and Gapdh were purchased from Applied Biosystems (Applied Biosystems, Foster City, CA, USA). All PCRs were performed in duplicate, and mRNA fold changes were calculated by the ΔΔCt method using Gapdh as internal reference.

Western blot analysis

After sacrificing the animals, cardiac tissue was immediately snap frozen in liquid nitrogen. Mouse hearts were lysed with ice-cold lysis buffer (Thermo Fisher Scientific, Rockford, IL, USA) supplemented with complete protease and phosphatase inhibitor cocktail (Thermo Fisher Scientific, Rockford, IL, USA). After centrifugation at 10,000 rpm for 5 min, 30 μg of proteins were boiled in Roti-Load1 Buffer (Carl Roth GmbH, Karlsruhe, Germany) at 100°C for 10 min. Proteins were separated on SDS-polyacrylamide gels and transferred to PVDF membranes. The membranes were incubated overnight at 4°C with goat anti-CTGF antibody (diluted 1:400, Santa Cruz Biotechnology, Santa Cruz, CA, USA) or rabbit anti-GAPDH antibody (diluted 1:1,000, Cell Signaling, Danvers, MA, USA) and then with secondary anti-goat HRP-conjugated antibody (diluted 1:2,000, Santa Cruz Biotechnology, Santa Cruz, CA, USA) or secondary anti-rabbit HRP-conjugated antibody (diluted 1:1,000, Cell Signaling, Danvers, MA, USA) for 1 h at RT. For loading controls, the membranes were stripped in stripping buffer (Carl Roth GmbH, Karlsruhe, Germany) at 56°C for 5 min. Antibody binding was detected with the ECL detection reagent (Amersham, Freiburg, Germany) and bands were quantified using Quantity One Software (Bio-Rad, München, Germany).

Isolation of adult cardiomyocytes

Adult cardiomyocytes were isolated from 8- to 10-week-old *sgk1*$^{-/-}$ and *sgk1*$^{+/+}$ mice as described [34] with minor modifications. In one study group, animals were pretreated with 1 week of transverse aortic constriction. Briefly, hearts were excised and retrogradely perfused by a perfusion buffer containing in mmol: NaCl 113, KCl 4.7, KH_2PO_4 0.6, Na_2HPO_4 0.6, $MgSO_4$·7H2O 1.2, phenol red 0.032, $NaHCO_3$ 12, $KHCO_3$ 10, Hepes 10, taurine 30, 2,3 butanedione-monoxime 10, glucose 5.5 (Sigma-Aldrich, Hamburg, Germany) at 37°C. After 2–3 min, perfusion was switched to perfusion buffer with added digestive enzymes 0.25 mg/ml liberase DH (Roche, Grenzach-Wyhlen, Germany) and 0.14 mg/ml trypsin (GIBCO/Invitrogen, Darmstadt, Germany) followed by careful dissection of the digested heart tissue. Buffer Ca^{2+} content was slowly adjusted to 1.2 mM. After isolation procedure, cardiomyocytes were plated on laminin-coated glass coverslips in plating medium [MEM medium (GIBCO/Invitrogen, Darmstadt, Germany) containing 5% BCS, 100 U/ml penicillin 10 mM 2,3 butanedione-monoxime and 2 mM L-glutamine]. After 1 h, cells were cultured in serum-free MEM medium containing 0.1 mg/ml BSA, 100 U/ml penicillin and 2 mM L-glutamine. Cardiomyocytes were allowed to settle for 1 h at 37°C and 2% CO2. Immediately after isolation, rod shaped myocytes were used for determination of Nhe activity.

Intracellular pH

For digital imaging of cytosolic pH (pH_i), the cells were incubated in a HEPES-buffered Ringer solution containing 10 μM BCECF-AM (Molecular Probes, Leiden, The Netherlands) for 15 min at 37°C [86]. After loading, the chamber was flushed for 5 min with Ringer solution to remove any deesterified dye. The perfusion chamber was mounted on the stage of an inverted microscope (Zeiss Axiovert 135), which was used in the epifluorescence mode with a 40× oil immersion objective (Zeiss Neoplan, Germany). BCECF was successively excited at 490/10 and 440/10 nm, and the resultant fluorescent signal was monitored at 535/10 nm using an intensified charge-coupled device camera (Proxitronic, Germany) and specialized computer software (Metafluor, USA) [85]. Cells were outlined and monitored during the course of the measurements. The results from each cell were averaged and taken for final analysis. Intensity ratio (490/440) data were converted into pH_i values using the high-K^+/nigericin calibration technique [94]. To this end, the cells were perfused at the end of each experiment for 5 min with standard high-K^+/nigericin (10 μg/ml) solution (pH 7.0). The intensity ratio data thus obtained were converted into pH values using the r_{max}, r_{min}, pK_a values previously generated from calibration experiments to generate a standard nonlinear curve (pH range 5–8.5).

For acid loading, cells were transiently exposed to a solution containing 20 mM NH_4Cl leading to initial alkalinization of cytosolic pH (pH_i) due to entry of NH_3 and binding of H^+ to form NH_4^+ [83]. The acidification of cytosolic pH upon removal of ammonia allowed calculating the mean intrinsic buffering power (β) of the cells [83]. Assuming that NH_4^+ and NH_3 are in equilibrium in

cytosolic and extracellular fluid and that ammonia leaves the cells as NH_3:

$$\beta = \Delta[NH_4^+]_i/\Delta pH_i,$$

where ΔpH_i is the decrease of cytosolic pH (pH_i) following ammonia removal and $\Delta[NH_4^+]_i$ is the decrease of cytosolic NH_4^+ concentration, which is identical to the concentration of $[NH_4^+]_i$ immediately before the removal of ammonia. The pK for NH_4^+/NH_3 is 8.9 [17] and at an extracellular pH (pH_o) of 7.4 the NH_4^+ concentration in extracellular fluid ($[NH_4^+]_o$) is 19.37 $[20/(1 + 10^{pH_o - pK})]$. The intracellular NH_4^+ concentration ($[NH_4]_i$) was calculated from [84].

$$[NH_4]_i = 19.37 \times 10^{pH_o - pH_i}.$$

The calculation of the buffer capacity required that NH_4^+ exits completely. After the initial decline, pH_i indeed showed little further change in the absence of Na^+, indicating that there was no relevant further exit of NH_4^+.To calculate the ΔpH/min during re-alkalinization, a manual linear fit was placed over a narrow pH range (pH 6.7–6.9) which could be applied to all measured cells.

The solutions were composed of (in mM): standard Hepes: 115 NaCl, 5 KCl, 1 $CaCl_2$, 1.2 $MgSO_4$, 2 NaH_2PO_4 10 glucose, 32.2 Hepes; sodium-free Hepes: 132.8 NMDG Cl, 3 KCl, 1 $CaCl_2$, 1.2 $MgSO_4$, 2 KH_2PO_4, 32.2 Hepes, 10 mannitol, 10 glucose (for sodium-free ammonium chloride 10 mM NMDG and mannitol were replaced with 20 mM NH_4Cl); high K^+ for calibration 105 KCl, 1 $CaCl_2$, 1.2 $MgSO_4$, 32.2 Hepes, 10 mannitol, 10 μg/ml nigericin. The pH of the solutions was titrated to 7.4 or 7.0 with HCl/NaOH, HCl/NMDG and HCl/KOH, respectively, at 37°C.

Statistics

Data are provided as mean ± SEM, n represents the number of independent experiments. Statistics was calculated with SPSS software. All data were tested for significance using Student's unpaired two-tailed t test or ANOVA following post hoc analysis and only results with $p < 0.05$ were considered statistically significant.

Results

A first series of experiments explored whether transverse aortic constriction (TAC) modifies Sgk1 transcription. As a result, a 1-week TAC treatment increased the Sgk1 transcript levels, which approached 1.06 ± 0.18 a.u. in sham-treated mice ($n = 5$) and 1.95 ± 0.22 a.u. ($n = 5$) in TAC-treated animals. To determine the impact of Sgk1 on cardiac remodeling, pressure overload by TAC was induced in gene targeted mice lacking functional Sgk1 ($sgk1^{-/-}$) as well as in their wild-type controls ($sgk1^{+/+}$). After 1 week of TAC treatment, aortic pressure was similarly elevated in $sgk1^{-/-}$ mice (128 ± 8 vs. sham 88 ± 2 mmHg, $p < 0.01$; $n = 3$–4) and $sgk1^{+/+}$ mice (129 ± 6 vs. sham 89 ± 6 mmHg, $p < 0.01$; $n = 4$). No significant difference was found between the genotypes.

TAC treatment for 1 week induced a hypertrophic response of $sgk1^{+/+}$ and $sgk1^{-/-}$ mouse hearts, which was slightly, but significantly ($p < 0.01$) blunted in the $sgk1^{-/-}$ hearts (Fig. 1). Heart weight was significantly ($p < 0.001$) increased in TAC-treated $sgk1^{+/+}$ mice (0.20 ± 0.01 g; $n = 7$) compared to sham-treated $sgk1^{+/+}$ mice (0.13 ± 0.01 g; $n = 6$). In $sgk1^{-/-}$ mice heart weight following TAC treatment was only slightly higher (0.16 ± 0.01 g, $n = 8$) than in sham-treated animals (0.13 ± 0.01 g, $n = 6$; $p < 0.01$). Similar results were obtained for the heart weight to tibia length ratio, which was significantly ($p < 0.001$) increased by TAC treatment in $sgk1^{+/+}$ mice, an effect again significantly ($p < 0.01$) blunted in $sgk1^{-/-}$ mice. The heart weight to body weight ratio showed again similar results (data not shown). No significant differences could be observed between sham-treated $sgk1^{+/+}$ and $sgk1^{-/-}$ hearts.

As illustrated in Fig. 1, after 5 weeks of pressure overload, heart weight was again significantly ($p < 0.05$) higher in $sgk1^{+/+}$ mice (0.21 ± 0.01 g, $n = 8$) than in $sgk1^{-/-}$ mice (0.18 ± 0.02 g, $n = 8$). The increase of heart weight to body weight ratio (data not shown) and heart weight to tibia length ratio (Fig. 1) in $sgk1^{+/+}$ mice was again significantly ($p < 0.05$) blunted in $sgk1^{-/-}$ mice. Again, no difference was observed between sham-treated $sgk1^{+/+}$ and $sgk1^{-/-}$ mice. In $sgk1^{+/+}$ mice, the increased heart weight after TAC treatment was accompanied by a significantly ($p < 0.01$) increased lung weight (0.120 ± 0.008 g, $n = 5$; Fig. 1), when compared to sham-treated $sgk1^{+/+}$ mice (0.083 ± 0.006 g, $n = 4$). No significant increase in lung weight was observed in $sgk1^{-/-}$ mice after 5 weeks TAC treatment (0.091 ± 0.002 g, $n = 5$) compared to sham treated in $sgk1^{-/-}$ mice (0.090 ± 0.008 g, $n = 4$). Along these lines the lung weight was significantly ($p < 0.01$) smaller in $sgk1^{-/-}$ mice than in $sgk1^{+/+}$ mice. Lung weight to tibia length ratio revealed similar results (Fig. 1).

TAC treatment increased left ventricular Anp transcript levels. This increase was significantly ($p < 0.01$) more pronounced in the hearts of $sgk1^{+/+}$ mice compared to $sgk1^{-/-}$ hearts (Fig. 2). Similar observations were made on Bnp expression in cardiac tissue. Again, Bnp transcript levels were increased by TAC treatment, an effect significantly ($p < 0.01$) blunted in $sgk1^{-/-}$ mice compared to $sgk1^{+/+}$ mice (Fig. 2). TAC treatment further increased within 1 week Collagen I and Collagen III transcript levels. The transcript levels of both Collagen I and Collagen III were significantly ($p < 0.01$) lower in $sgk1^{-/-}$ hearts. Connective tissue growth factor (Ctgf) expression was

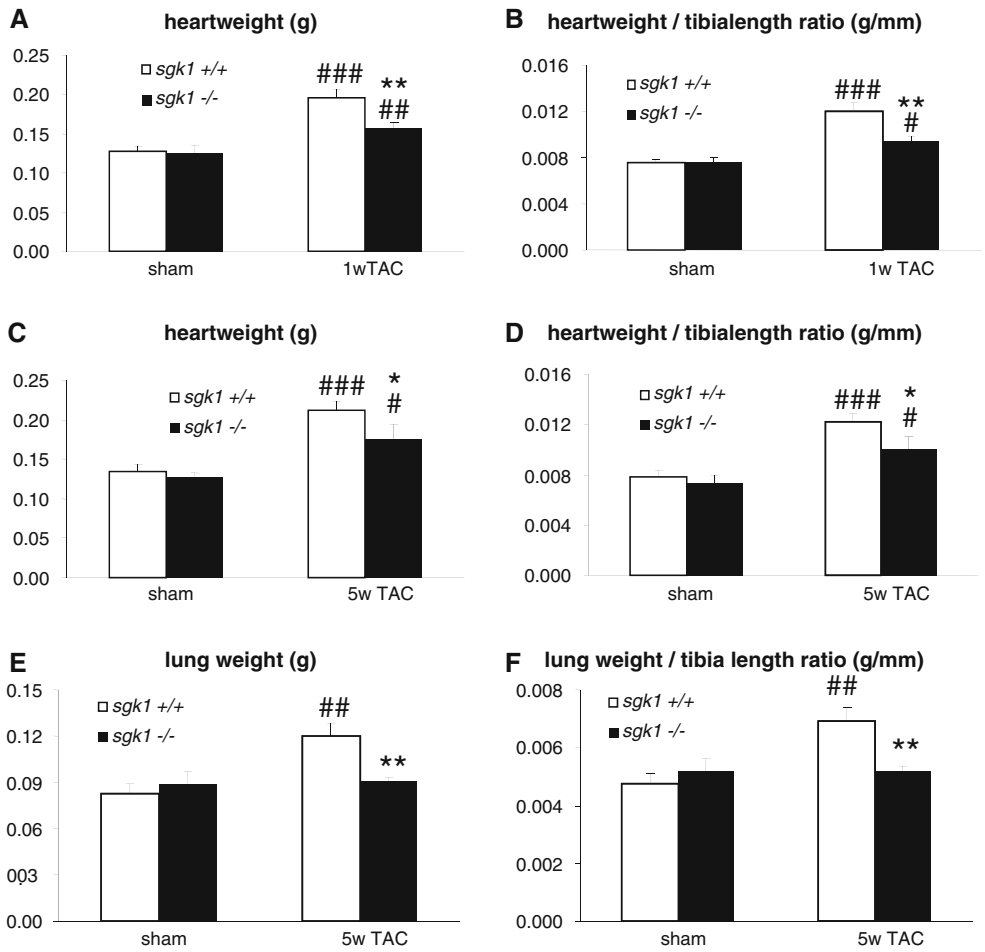

Fig. 1 Heart and lung weight in $sgk1^{+/+}$ and $sgk1^{-/-}$ mice after transverse aortic constriction/sham procedure. **a**, **b** Arithmetic mean ± SEM of heart weight (**a** g) and heart weight to tibia length ratio (**b** g/mm) in Sgk1 knockout mice ($sgk1^{-/-}$, *black bars*) and respective wild-type mice ($sgk1^{+/+}$, *white bars*) with sham (control, *left bars*, $n = 6$/group) or with (TAC, *right bars*, $n = 7$–8/group) transverse aortic constriction for 1 week. **c**, **d** Arithmetic mean ± SEM of heart weight (g) (**c**) and heart weight to tibia length ratio (g/mm) (**d**) in Sgk1 knockout mice ($sgk1^{-/-}$, *black bars*) and respective wild-type mice ($sgk1^{+/+}$, *white bars*) with sham (control, *left bars*, $n = 6$/group) or with (TAC, *right bars*, $n = 8$/group) transverse aortic constriction for 5 weeks. **e**, **f** Arithmetic mean ± SEM of lung weight (g) (**e**) or lung weight to tibia length ratio (g/mm) (**f**) in Sgk1 knockout mice ($sgk1^{-/-}$, *black bars*) and respective wild-type mice ($sgk1^{+/+}$, *white bars*) with sham (control, *left bars*, $n = 4$/group) or with (TAC, *right bars*, $n = 5$/group) transverse aortic constriction for 5 weeks. $^{\#}p < 0.05$, $^{\#\#}p < 0.01$, $^{\#\#\#}p < 0.001$ indicates statistically significant difference from respective control; $^{*}p < 0.05$, $^{**}p < 0.01$, $^{***}p < 0.001$ indicates statistically significant difference from respective $sgk1^{+/+}$ mice

significantly ($p < 0.001$) increased in both genotypes after TAC, yet the increase was again significantly blunted in $sgk1^{-/-}$ mice on transcript ($p < 0.001$) and protein ($p < 0.05$) level (Fig. 2).

A further series of experiments explored the effect of pressure overload on Nhe1 transcript levels. As illustrated in Fig. 3, TAC treatment significantly ($p < 0.01$) increased Nhe1 mRNA levels in $sgk1^{+/+}$ mice but not in $sgk1^{-/-}$ mice. Both, with sham or with TAC treatment, Nhe1 transcript levels were significantly ($p < 0.05$ and $p < 0.001$, respectively) lower in $sgk1^{-/-}$ mice than in $sgk1^{+/+}$ mice. Similar results as in sham-treated mice were observed in untreated mice (data not shown). In addition, Spp1 mRNA expression was significantly increased, while Pgc1a was significantly reduced in TAC treated $sgk1^{+/+}$ mice (both $p < 0.001$). Both, the upregulation of Spp1 expression ($p < 0.01$) and the downregulation of Pgc1a expression ($p < 0.05$), were significantly blunted in $sgk1^{-/-}$ mice (Fig. 3).

In a further series of experiments cytosolic pH and Nhe activity were measured in primary isolated cardiomyocytes (Table 1). Cytosolic pH tended to be lower in $sgk1^{-/-}$ cardiomyocytes than in $sgk1^{+/+}$ cardiomyocytes, a difference, however, not reaching statistical significance (Fig. 4). 1 week of TAC treatment significantly ($p < 0.05$) increased cytosolic pH in $sgk1^{+/+}$ cardiomyocytes but not in $sgk1^{-/-}$ cardiomyocytes. Accordingly, following TAC treatment, cytosolic pH was significantly ($p < 0.001$) lower

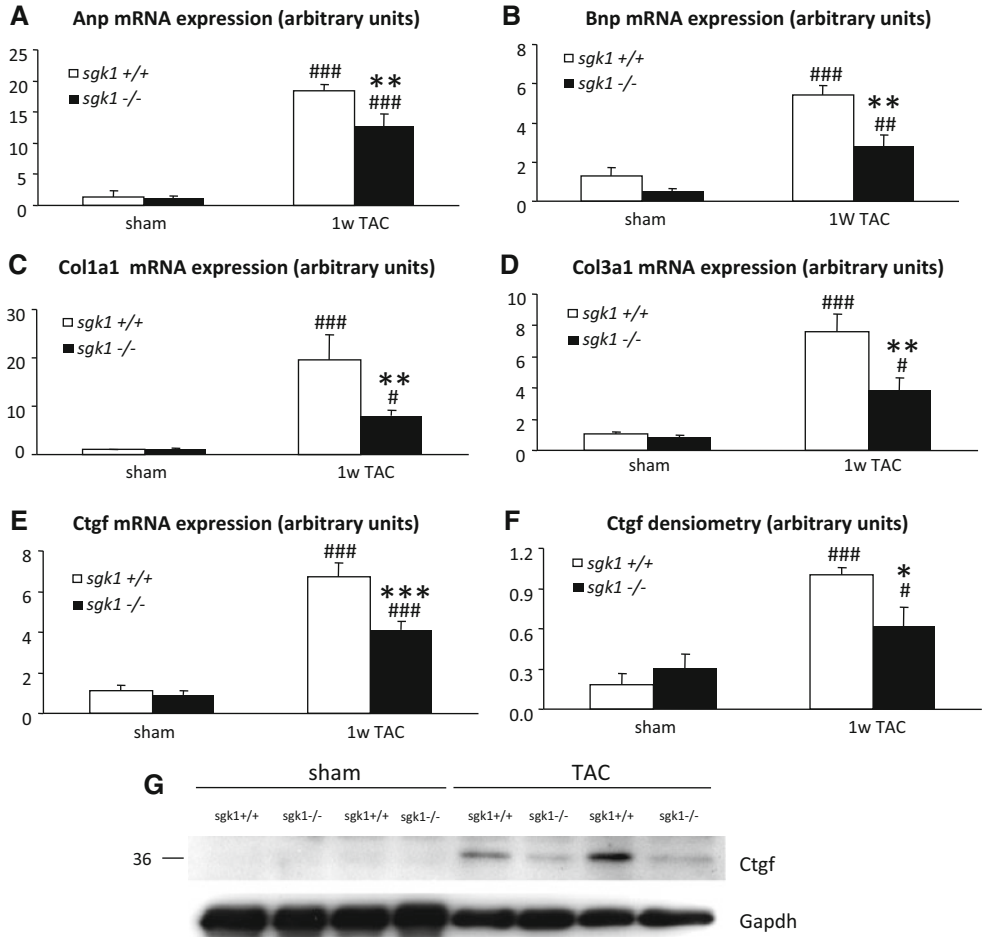

Fig. 2 Cardiac Anp/Bnp and fibrosis marker expression in $sgk1^{+/+}$ and $sgk1^{-/-}$ mice after transverse aortic constriction/sham procedure **a–e** Arithmetic mean ± SEM ($n = 5$–8/group) of mRNA expression levels encoding atrial natriuretic peptide (Anp; **a**), brain natriuretic peptide (Bnp; **b**), Collagen I (**c**), Collagen III (**d**) and Ctgf (**e**) in cardiac tissue from Sgk1 knockout mice ($sgk1^{-/-}$, *black bars*) and respective wild-type mice ($sgk1^{+/+}$, *white bars*) with sham operation (control, *left bars*) or with (TAC, *right bars*) transverse aortic constriction for 1 week. **f**, **g** Densitometry ($n = 4$; **f**) and representative original blots (**g**) of CTGF protein levels in cardiac tissue from Sgk1 knockout mice ($sgk1^{-/-}$, *black bars*) and respective wild-type mice ($sgk1^{+/+}$, *white bars*) with sham (control, *left bars*) or with (TAC, *right bars*) transverse aortic constriction procedure for 1 week. $^{\#}p < 0.05$, $^{\#\#}p < 0.01$, $^{\#\#\#}p < 0.001$ indicates statistically significant difference from respective control; $^{*}p < 0.05$, $^{**}p < 0.01$, $^{***}p < 0.001$ indicates statistically significant difference from respective $sgk1^{+/+}$ mice

in $sgk1^{-/-}$ cardiomyocytes than in $sgk1^{+/+}$ cardiomyocytes.

Prior to aortic banding NHE activity tended to be lower in $sgk1^{-/-}$ mice than in $sgk1^{+/+}$ mice, a difference, however, not reaching statistical significance ($p < 0.07$). TAC treatment within 1 week significantly ($p < 0.01$) increased the calculated NHE activity in $sgk1^{+/+}$ cardiomyocytes but not in $sgk1^{-/-}$ cardiomyocytes. Accordingly, following TAC treatment the NHE activity was significantly lower ($p < 0.001$) in $sgk1^{-/-}$ cardiomyocytes than in $sgk1^{+/+}$ cardiomyocytes.

In a next series of experiments, the ejection fraction as a measure of cardiac function was determined by cardiac magnetic cine resonance imaging (Table 2; Fig. 5). Without TAC treatment, the ejection fraction was similar in $sgk1^{-/-}$ mice and in $sgk1^{+/+}$ mice. Within 1 week of TAC treatment the ejection fraction decreased strongly and significantly ($p < 0.001$) from 62.9 ± 2.7% to 42.9 ± 4.1% in $sgk1^{+/+}$ mice. The ejection fraction continued to slightly decline over the observation period and showed a further decrease following a 3 weeks (39.0 ± 3.8%) and 5 weeks (34.7 ± 2.4%) TAC treatment. TAC treatment tended to slightly decrease the ejection fraction in $sgk1^{-/-}$ mice (from 61.2 ± 2.0 to 55.1 ± 3.2% within 5 weeks), an effect, however, not reaching statistical significance (Fig. 5). Accordingly, following TAC treatment, the ejection fraction was significantly ($p < 0.001$) larger in $sgk1^{-/-}$ mice than in $sgk1^{+/+}$ mice.

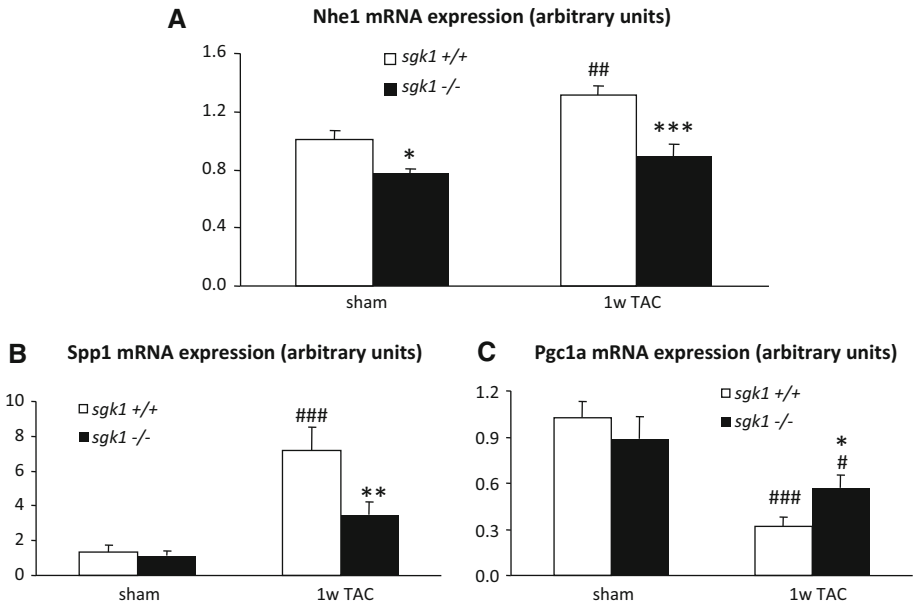

Fig. 3 Cardiac expression of Nhe1 and Nhe1 targets in left ventricular tissue after sham operation or transverse aortic constriction Arithmetic mean ± SEM ($n = 5$–9) of Nhe1 (**a**), Spp1 (**b**) and Pgc1a (**c**) mRNA levels in cardiac tissue from Sgk1 knockout mice ($sgk1^{-/-}$, *black bars*) and respective wild-type mice ($sgk1^{+/+}$, *white bars*) with sham (control, *left bars*) or with (TAC, *right bars*) transverse aortic constriction procedure for 1 week. $^{\#\#}p < 0.01$, $^{\#\#\#}p < 0.001$ indicates statistically significant difference from respective control, $^{*}p < 0.05$, $^{**}p < 0.01$, $^{***}p < 0.001$ indicates statistically significant difference from respective $sgk1^{+/+}$ mice

Table 1 Cytosolic pH (ΔpH_i), buffer capacity and sodium-independent pH recovery in cardiac myocytes from Sgk1 knockout mice ($sgk1^{-/-}$) and respective wild-type mice ($sgk1^{+/+}$) without (baseline) and with (TAC) prior left ventricular pressure overload by aortic banding

	Intracellular pH (units)	Buffer capacity (mM/pH unit)	Sodium-independent pH recovery (Δ pH units/min)	Sodium-dependent pH recovery (NHE activity, Δ pH units/min)
Baseline $sgk1^{+/+}$	7.26 ± 0.03	19.92 ± 3.40	−0.004 ± 0.005	0.069 ± 0.007
Baseline $sgk1^{-/-}$	7.18 ± 0.03	21.56 ± 2.81	−0.020 ± 0.008	0.041 ± 0.007^{+}
TAC $sgk1^{+/+}$	7.35 ± 0.02$^{\#}$	18.09 ± 2.94	−0.015 ± 0.004	0.098 ± 0.007$^{\#\#}$
TAC $sgkt1^{-/-}$	7.14 ± 0.02***	23.20 ± 2.00	−0.015 ± 0.006	0.050 ± 0.005***

All values calculated from 5 independent experiments

$^{\#}$ $p < 0.05$; $^{\#\#}$ $p < 0.01$: statistically significant difference from baseline values; *** $p < 0.001$: statistically significant difference from respective $sgk1^{+/+}$ mice; $^{+}$ indicates difference $p < 0.07$ from respective $sgk1^{+/+}$ mice

Further experiments were performed to elucidate cardiac glucose uptake utilizing ^{18}F-labeled glucose ([^{18}F]FDG) measured by PET imaging (Fig. 6). Prior to TAC treatment, the glucose uptake tended to be higher in $sgk1^{-/-}$ mice than in $sgk1^{+/+}$ mice, a difference, however, not reaching statistical significance. Within 1 week, the TAC treatment significantly ($p < 0.001$) increased cardiac glucose uptake in $sgk1^{+/+}$ mice. TAC treatment significantly ($p < 0.05$) increased cardiac glucose uptake as well in $sgk1^{-/-}$ mice, an effect, however, significantly blunted as compared to $sgk1^{+/+}$ mice. As a result, following TAC treatment, the glucose uptake was significantly ($p < 0.01$ after 1 week and $p < 0.001$ after 5 weeks, respectively) lower in $sgk1^{-/-}$ mice than in $sgk1^{+/+}$ mice (Fig. 6).

Discussion

The present study reveals that the lack of Sgk1 reduces the influence of pressure overload by transverse aortic constriction (TAC) on cardiac function, Nhe1 expression and several indicators of cardiac remodeling. Hearts from gene targeted mice lacking functional Sgk1 ($sgk1^{-/-}$) appear to be at least partly protected against the deleterious effects of excessive cardiac workload. In the wild-type mice ($sgk1^{+/+}$) a strong effect of pressure overload was visible after 1 week, suggesting a particular sensitivity of the mouse strain to TAC. The changes induced by pressure overload were not abrogated, but significantly blunted in $sgk^{-/-}$ mice. The effects of TAC in $sgk1^{-/-}$ mice are due to mechanisms other

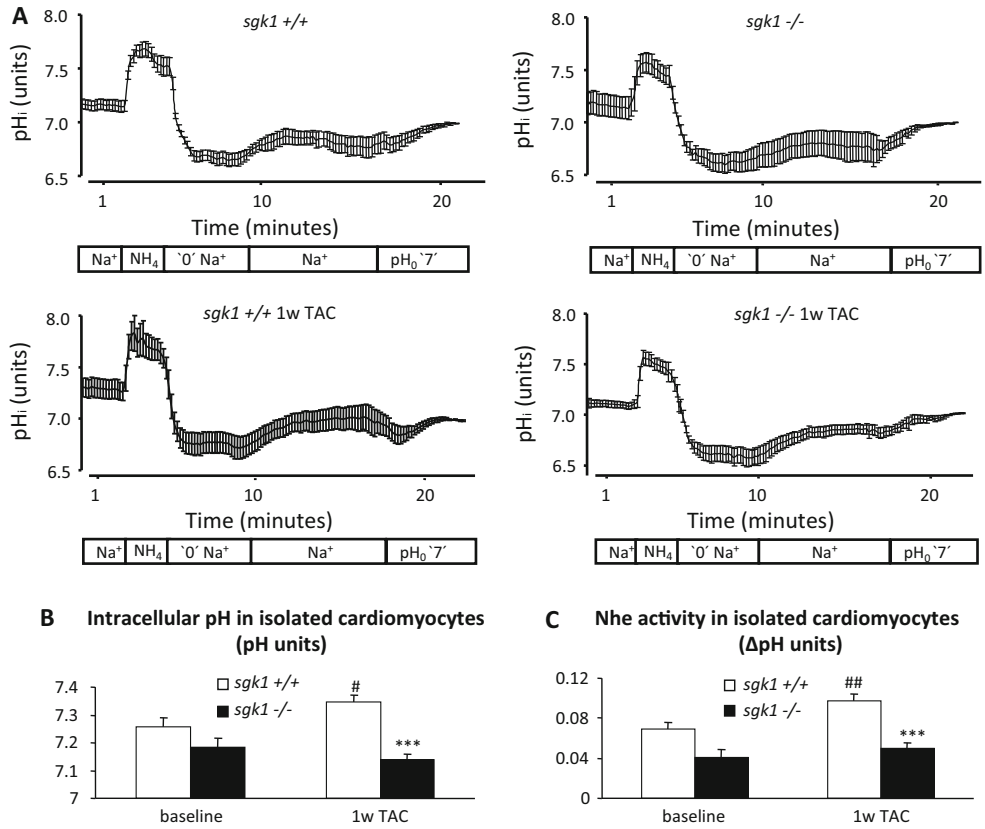

Fig. 4 NHE activity in cardiomyocytes isolated from $sgk1^{+/+}$ and $sgk1^{-/-}$ hearts with or without prior transverse aortic constriction Alterations of cytosolic pH (pH_i) in cardiomyocytes isolated from Sgk1 knockout mice ($sgk1^{-/-}$) and respective wild-type mice ($sgk1^{+/+}$) following an ammonium pulse. To load the cells with H^+, 20 mM NH_4Cl was added and Na^+ removed (replaced by NMDG) in a first step (see bars below each original tracing), NH_4Cl removed in a second step, Na^+ added in a third step and nigericin (pH_o 7.0) applied in a fourth step to calibrate each individual experiment. **a** Time-dependent changes ± SEM of cytosolic pH in typical experiments in cardiomyocytes derived from $sgk1^{+/+}$ (*left panels*) and $sgk1^{-/-}$ (*right panels*) hearts without (*upper panels*) and with (*lower panels*) prior transverse aortic constriction (TAC) for 1 week. **b** Arithmetic mean ± SEM ($n = 5$ independent experiments) of cytosolic pH prior to the ammonium pulse (pH_i) in $sgk1^{+/+}$ (*white bars*) or $sgk1^{-/-}$ (*black bars*) cardiomyocytes from hearts without (control, *left bars*) or with (TAC, *right bars*) prior transverse aortic constriction for 1 week. **c** Arithmetic mean ± SEM ($n = 5$ independent experiments) of Na^+-dependent recovery of cytosolic pH (ΔpH/min) following an ammonium pulse in cardiomyocytes from $sgk1^{+/+}$ (*white bars*) or $sgk1^{-/-}$ (*black bars*) mice without (control, *left bars*) or with (TAC, *right bars*) prior transverse aortic constriction for 1 week. $^{\#}p < 0.05$, $^{\#\#}p < 0.01$ indicates statistically significant difference from respective control; $^{***}p < 0.001$ indicates statistically significant difference from respective $sgk1^{+/+}$ mice

than SGK1. Along these lines cardiomyocyte hypertrophy was increased in cardiomyocytes transfected with constitutively active SGK1 [10]. SGK1 may not be necessary for induction of cardiomyocyte hypertrophy, but may augment the hypertrophic response [63]. According to the previous and the present observations SGK1 contributes to, but does not fully account for the hypertrophy and cardiac remodeling during excessive workload.

SGK1 is at least partially effective by regulating Na^+/H^+ exchanger activity. The Na^+/H^+ exchanger 1 is the major NHE isoform in the heart [47, 80]. The cardiac NHE1 is contributing to various pathological conditions, including myocardial reperfusion injury [98]. NHE1 activity is also increased in failing human hearts [101]. NHE1 activity is at least partially effective by augmenting the Na^+ entry into anoxic myocardium [23] and thereby reversing Na^+/Ca^{2+} exchange and thus increasing intracellular Ca^{2+} content [6]. The NHE1 activity contributes to cardiac hypertrophy [61, 65, 66, 100]. Accordingly, cardiac hypertrophy and its progression to heart failure can be strongly reduced by NHE1 inhibitors [1, 24, 60]. Moreover, NHE1 stimulation alone is sufficient to trigger cardiac hypertrophy and heart failure [70]. NHE1 exerts its deleterious effects in cardiac pathology by its transport activity [67]. The mechanisms underlying upregulation of NHE1 during cardiac hypertrophy and heart failure remained incompletely understood.

Important targets of activated NHE1 in the pathophysiology of cardiac hypertrophy include Spp1 and Pgc1a [100]. Accordingly, the increase of Spp1 and the decrease of Pgc1a transcript levels were blunted in $sgk1^{-/-}$ mice, paralleling the reduced NHE1 activity in

Table 2 Cardiac function parameters measured during MRI scan

	sgk1$^{+/+}$ baseline	*sgk1*$^{-/-}$ baseline	*sgk1*$^{+/+}$ 1w TAC	*sgk1*$^{-/-}$ 1w TAC	*sgk1*$^{+/+}$ 3w TAC	*sgk1*$^{-/-}$ 3w TAC	*sgk1*$^{+/+}$ 5w TAC	*sgk1*$^{-/-}$ 5w TAC
Ejection fraction (%)	62.9 ± 2.7	61.2 ± 2.0	42.9 ± 4.1$^{\#\#\#}$	61.3 ± 2.8***	39.0 ± 3.8$^{\#\#\#}$	55.2 ± 1.4***	34.7 ± 2.4$^{\#\#\#}$	55.1 ± 3.2***
LV vol. diastolic (μl)	52.2 ± 3.0	51.2 ± 3.2	59.7 ± 3.3	52.4 ± 5.4	59.6 ± 2.4	51.5 ± 3.5	63.4 ± 3.3$^{\#}$	54.4 ± 3.8
LV vol. systolic (μl)	19.7 ± 2.3	19.9 ± 1.6	34.5 ± 3.9$^{\#\#}$	21.0 ± 3.9**	36.5 ± 3.1$^{\#\#\#}$	23.2 ± 2.2**	43.7 ± 3.5$^{\#\#\#}$	25.0 ± 3.4**
LV diameter systolic (mm)	2.37 ± 0.13	2.41 ± 0.20	2.83 ± 0.08	2.37 ± 0.25	3.30 ± 0.14$^{\#\#}$	2.62 ± 0.14**	3.62 ± 0.21$^{\#\#}$	2.51 ± 0.20***
Heart rate (bpm)	496 ± 27	502 ± 22	496 ± 20	440 ± 17	471 ± 34	429 ± 17$^{\#}$	471 ± 10	442 ± 24
Respiratory rate (bpm)	84 ± 8	68 ± 6	105 ± 4$^{\#}$	88 ± 5	114 ± 5$^{\#\#}$	101 ± 6$^{\#\#}$	102 ± 10	84 ± 11

$^{\#}$ $p < 0.05$, $^{\#\#}$ $p < 0.01$, $^{\#\#\#}$ $p < 0.001$ indicates statistically significant difference from baseline values, * $p < 0.05$, ** $p < 0.01$, *** $p < 0.001$ indicates statistically significant difference from respective *sgk1*$^{+/+}$ mice

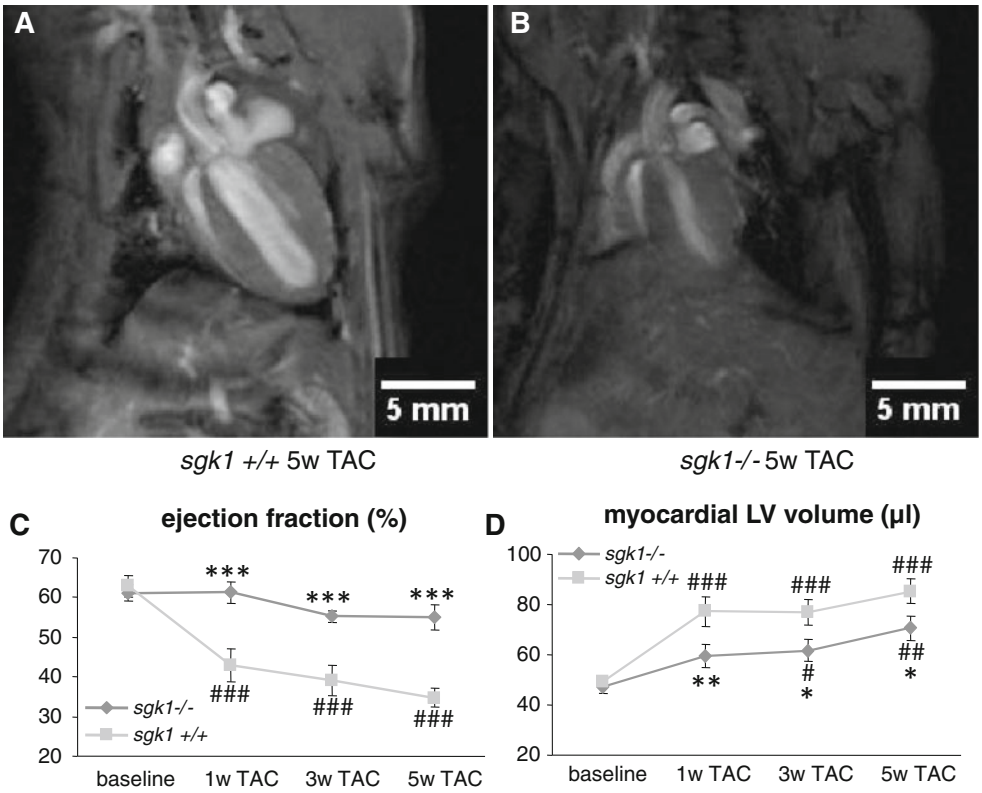

Fig. 5 Cardiac function in *sgk1*$^{+/+}$ and *sgk1*$^{-/-}$ mice after transverse aortic constriction. **a**, **b** Representative images from cardiac cine magnetic resonance imaging. Example images of end-systolic longitudinal axis scan of *sgk1*$^{+/+}$ (**a**) and *sgk1*$^{-/-}$ (**b**) mouse hearts 5 weeks after TAC procedure. *Scale bar* 5 mm. **c** Arithmetic mean ± SEM ($n = 5$–6/group) of ejection fraction (%) of *sgk1*$^{+/+}$ (*squares*, *gray line*) and *sgk1*$^{-/-}$ (*rhombi*, *black line*) mouse hearts measured by cardiac cine magnetic resonance imaging at baseline, 1, 3 and 5 weeks after TAC procedure. **d** Arithmetic mean ± SEM ($n = 5$–6/group) of myocardial volume of the left ventricle (μl) of *sgk1*$^{+/+}$ (*squares*, *gray line*) and *sgk1*$^{-/-}$ (*rhombi*, *black line*) mouse hearts measured in diastole by cardiac cine magnetic resonance imaging at baseline, 1, 3 and 5 weeks after TAC procedure. $^{\#}p < 0.05$, $^{\#\#}p < 0.01$, $^{\#\#\#}p < 0.001$ indicates statistically significant difference from baseline measurements; $^{*}p < 0.05$, $^{***}p < 0.001$ indicates statistically significant difference from respective *sgk1*$^{+/+}$ mice

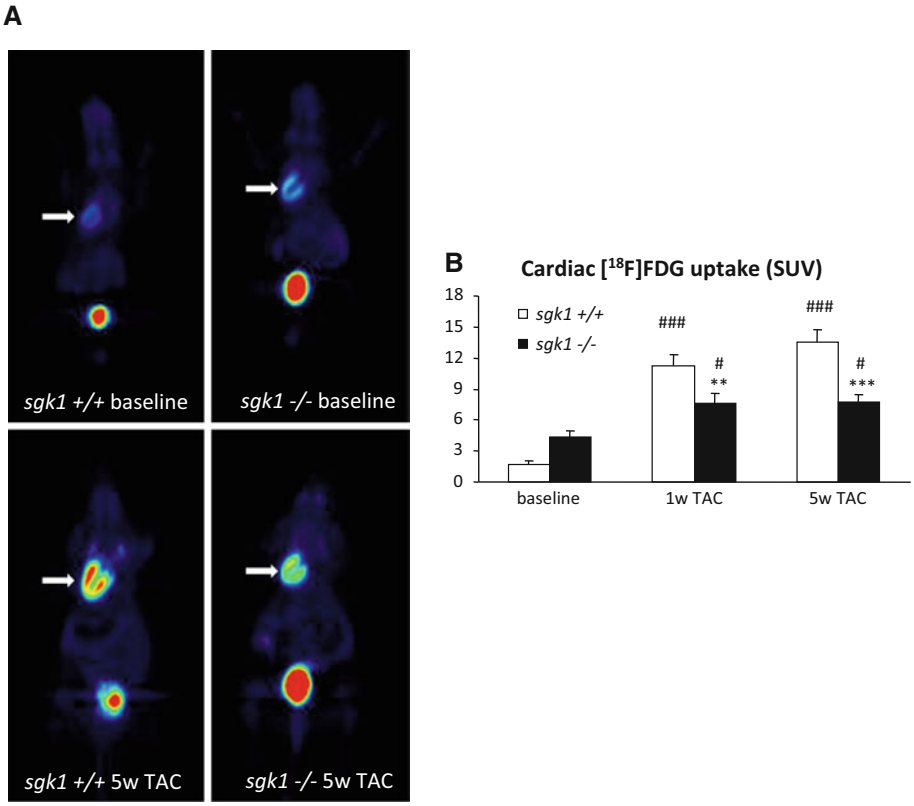

Fig. 6 Loss of Sgk1 blunts metabolic remodeling after TAC. **a** Example images of PET imaging depicting [^{18}F]FDG uptake of $sgk1^{+/+}$ (*left column*) and $sgk1^{-/-}$ (*right column*) mice before (*upper row*) and 5 weeks after TAC procedure (*lower row*). *Arrows* added to indicate murine heart. **b** Arithmetic mean ± SEM (n = 5–6/group) of ^{18}F-labeled glucose uptake (standardized uptake value, SUV) in cardiac tissue of Sgk1 knockout mice ($sgk1^{-/-}$, *black bars*) and respective wild-type mice ($sgk1^{+/+}$, *white bars*) at baseline and after transverse aortic constriction for 1 and 5 weeks, respectively. $^{\#}p < 0.05$, $^{\#\#\#}p < 0.001$ indicates statistically significant difference from respective control; ** $p < 0.01$, ***$p < 0.001$ indicates statistically significant difference from respective $sgk1^{+/+}$ mice

those mice. Due to the major role of Na^+/H^+ exchanger in cardiac pathophysiology, its regulation is of pathophysiological significance [28]. According to the present observations, SGK1 is a major determinant of NHE1 activity in the failing heart. SGK1-dependent NHE1 regulation is a possible mechanism for the partial cardioprotection in $sgk1^{-/-}$ mice.

However, SGK1 may not only be effective through NHE1. Instead, the kinase regulates a wide variety of transcription factors, such as NFκB [54], which may in turn influence the expression of further genes involved in cardiac hypertrophy and deterioration of cardiac function during aortic banding.

At least in theory, SGK1 could influence cardiac function by modifying blood volume [99], pulmonary vascular resistance [12] and/or peripheral blood pressure [54]. Accordingly, alterations of lung weight could have been modified by effects of SGK1 on pulmonary vascular function. However, SGK1 would be rather expected to increase pulmonary vascular resistance [12], which is not expected to increase the pulmonary weight. In the present experiments, no differences were observed in the maximal aortic blood pressure between $sgk1^{-/-}$ mice and $sgk1^{+/+}$ mice.

NHE activity is decreased, but not abolished in $sgk1^{-/-}$ mice. Thus, pharmacological inhibition of NHE1 may be more rigorously suppressed by NHE1 inhibitors than in the absence of SGK1 and pharmacological NHE1 inhibition may still have some effect in $sgk1^{-/-}$ mice.

SGK1 expression is stimulated by a variety of triggers including glucocorticoids [27], mineralocorticoids [18, 71, 89], 1,25-dyhydroxyvitamin D_3 ($1,25(OH)_2D_3$) [2], cell shrinkage [95], gonadotropins [7, 8, 35, 79], and TGFβ [58, 96]. In addition, SGK1 has been shown to be upregulated and activated after pressure overload induced heart failure [10]. SGK1 is activated through phosphatidylinositide 3 kinase (PI3K) and phosphoinositide-dependent kinase PDK1 [3, 4, 21, 31, 50, 53, 75]. Thus, under conditions of enhanced SGK1 expression, SGK1 could substantially contribute to PI3K-dependent signaling. PI3K has previously been shown to participate in the triggering of cardiac hypertrophy [9, 20, 36, 37, 74, 82, 102]. PI3K signaling is proposed to regulate the cardiac NHE1 [59]. During pressure overload, PI3K may

further activate AKT [69], which, however, has been shown to inhibit NHE1 [90] and thus hardly accounts for the increased NHE1 activity after pressure overload.

The stimulation of CTGF and Collagen I and III expression following TAC is significantly blunted in *sgk1*$^{-/-}$ mice, an observation pointing to a reduced fibrotic response of *sgk1*$^{-/-}$hearts. Previous studies already revealed the requirement for SGK1 in the induction of cardiac fibrosis by mineralocorticoids, an effect mediated by SGK1-dependent up-regulation of nuclear factor-κB (NF-κB) [92]. Intriguingly, NF-κB activity has also been shown to be suppressed upon NHE inhibition [72] and NF-κB activity is increased in Pgc1a knockout mice [22]. The SGK1-dependent stimulation of Na^+/H^+ exchanger activity is expected to increase cell volume [40, 55] thus fostering cell volume-dependent stimulation of net protein synthesis [39, 55]. Moreover, stimulation of Na^+/H^+ exchanger activity fosters NADPase activity [19, 32], which again parallels cardiac remodeling [68].

Heart failure is associated with a cardiac substrate switch from fatty acid oxidation to glycolysis [62]. *Sgk1*$^{-/-}$ mice show a reduced glucose uptake after pressure overload. Activation of NHE1 is associated with an increase of cardiac glycolysis [67, 88]. SGK1-dependent stimulation of Na^+/H^+ exchanger activity leads to cytosolic alkalinization which fosters the flux through glycolysis and thus glucose utilization [15].

In view of the protective role of SGK1 deficiency against cardiac hypertrophy and fibrosis, the question arises, whether or not effects of SGK1 may be exclusively negative. Generally, replacement of functional tissue by fibrotic tissue results in a decline of tissue-specific functions but by the same token decreases the energy demand and thus promotes survival of the tissue during energy depletion. Several other pathophysiologically relevant SGK1-dependent functions are similarly potentially positive. The SGK1-dependent increase of blood pressure [54], for instance, may foster physical performance during fight and flight and the stimulation of platelet function by SGK1 [16] is expected to decrease blood loss following injury. Thus, the pathophysiologically relevant molecular functions of SGK1 are not exclusively negative.

In conclusion, genetic knockout of Sgk1 protects against the stimulation of Na^+/H^+ exchanger activity following transverse aortic banding. The present observations thus disclose a novel player in the stimulation of cardiac remodeling following excessive workload. Hence, targeting SGK1 could be beneficial in the failing heart [57].

Acknowledgments We thank Maren Koenig (PET), Mareike Lehnhoff (PET), Funda Cay (PET) and Salvador Castaneda (MR) for outstanding technical support during the imaging measurements. Radiotracers were produced by the radiopharmacy group of the Department of Preclinical Imaging and Radiopharmacy at the University Hospital of Tübingen. We also thank Evi Faber and Klaudia Kloß for their valuable technical support. This work was supported by grants from the Deutsche Forschungsgemeinschaft (La315/4-5 and SFB-Transregio 19).

References

1. Aker S, Snabaitis AK, Konietzka I, Van De SA, Bongler K, Avkiran M, Heusch G, Schulz R (2004) Inhibition of the Na+/H+ exchanger attenuates the deterioration of ventricular function during pacing-induced heart failure in rabbits. Cardiovasc Res 63:273–282. doi:10.1016/j.cardiores.2004.04.014
2. Akutsu N, Lin R, Bastien Y, Bestawros A, Enepekides DJ, Black MJ, White JH (2001) Regulation of gene expression by 1α,25-dihydroxyvitamin D3 and its analog EB1089 under growth-inhibitory conditions in squamous carcinoma cells. Mol Endocrinol 15:1127–1139. doi:10.1210/me.15.7.1127
3. Alessi DR, Andjelkovic M, Caudwell B, Cron P, Morrice N, Cohen P, Hemmings BA (1996) Mechanism of activation of protein kinase B by insulin and IGF-1. EMBO J 15:6541–6551
4. Alessi DR, Cohen P (1998) Mechanism of activation and function of protein kinase B. Curr Opin Genet Dev 8:55–62. doi:10.1016/S0959-437X(98)80062-2
5. Alesutan IS, Ureche ON, Laufer J, Klaus F, Zurn A, Lindner R, Strutz-Seebohm N, Tavare JM, Boehmer C, Palmada M, Lang UE, Seebohm G, Lang F (2010) Regulation of the glutamate transporter EAAT4 by PIKfyve. Cell Physiol Biochem 25:187–194. doi:10.1159/000276569
6. Allen DG, Xiao XH (2003) Role of the cardiac Na+/H+ exchanger during ischemia and reperfusion. Cardiovasc Res 57:934–941. doi:10.1016/S0008-6363(02)00836-2
7. Alliston TN, Gonzalez-Robayna IJ, Buse P, Firestone GL, Richards JS (2000) Expression and localization of serum/glucocorticoid-induced kinase in the rat ovary: relation to follicular growth and differentiation. Endocrinology 141:385–395. doi:10.1210/en.141.1.385
8. Alliston TN, Maiyar AC, Buse P, Firestone GL, Richards JS (1997) Follicle stimulating hormone-regulated expression of serum/glucocorticoid-inducible kinase in rat ovarian granulosa cells: a functional role for the Sp1 family in promoter activity. Mol Endocrinol 11:1934–1949. doi:10.1210/me.11.13.1934
9. Alvin Z, Laurence GG, Coleman BR, Zhao A, Hajj-Moussa M, Haddad GE (2011) Regulation of L-type inward calcium channel activity by captopril and angiotensin II via the phosphatidyl inositol 3-kinase pathway in cardiomyocytes from volume-overload hypertrophied rat hearts. Can J Physiol Pharmacol 89:206–215. doi:10.1139/Y11-011
10. Aoyama T, Matsui T, Novikov M, Park J, Hemmings B, Rosenzweig A (2005) Serum and glucocorticoid-responsive kinase-1 regulates cardiomyocyte survival and hypertrophic response. Circulation 111:1652–1659. doi:10.1161/01.CIR.0000160352.58142.06
11. Baartscheer A (2006) Chronic inhibition of Na(+)/H(+)-exchanger in the heart. Curr Vasc Pharmacol 4:23–29. doi:10.2174/157016106775203117
12. Belaiba RS, Djordjevic T, Bonello S, Artunc F, Lang F, Hess J, Gorlach A (2006) The serum- and glucocorticoid-inducible kinase Sgk-1 is involved in pulmonary vascular remodeling: role in redox-sensitive regulation of tissue factor by thrombin. Circ Res 98:828–836. doi:10.1161/01.RES.0000210539.54861.27
13. Bisognano JD, Weinberger HD, Bohlmeyer TJ, Pende A, Raynolds MV, Sastravaha A, Roden R, Asano K, Blaxall BC, Wu SC, Communal C, Singh K, Colucci W, Bristow MR, Port DJ

(2000) Myocardial-directed overexpression of the human beta(1)-adrenergic receptor in transgenic mice. J Mol Cell Cardiol 32:817–830. doi:10.1006/jmcc.2000.1123
14. Bohmer C, Sopjani M, Klaus F, Lindner R, Laufer J, Jeyaraj S, Lang F, Palmada M (2010) The serum and glucocorticoid inducible kinases SGK1-3 stimulate the neutral amino acid transporter SLC6A19. Cell Physiol Biochem 25:723–732. doi:10.1159/000315092
15. Boiteux A, Hess B (1981) Design of glycolysis. Philos Trans R Soc Lond B Biol Sci 293:5–22. doi:10.1098/rstb.1981.0056
16. Borst O, Schmidt EM, Munzer P, Schonberger T, Towhid ST, Elvers M, Leibrock C, Schmid E, Eylenstein A, Kuhl D, May AE, Gawaz M, Lang F (2011) The serum- and glucocorticoid-inducible kinase 1 (SGK1) influences platelet calcium signaling and function by regulation of Orai1 expression in megakaryocytes. Blood doi:10.1182/blood-2011-06-359976 (in press)
17. Boyarsky G, Ganz MB, Sterzel RB, Boron WF (1988) pH regulation in single glomerular mesangial cells. II. Na+-dependent and -independent Cl(−)-HCO3-exchangers. Am J Physiol 255:C857–C869
18. Chen SY, Bhargava A, Mastroberardino L, Meijer OC, Wang J, Buse P, Firestone GL, Verrey F, Pearce D (1999) Epithelial sodium channel regulated by aldosterone-induced protein sgk. Proc Natl Acad Sci USA 96:2514–2519. doi:10.1073/pnas.96.5.2514
19. Cingolani HE, Ennis IL, Aiello EA, Perez NG (2011) Role of autocrine/paracrine mechanisms in response to myocardial strain. Pflugers Arch. doi:10.1007/s00424-011-0930-9 (in press)
20. Damilano F, Perino A, Hirsch E (2010) PI3K kinase and scaffold functions in heart. Ann NY Acad Sci 1188:39–45. doi:10.1111/j.1749-6632.2009.05081.x
21. Divecha N, Banfic H, Irvine RF (1991) The polyphosphoinositide cycle exists in the nuclei of Swiss 3T3 cells under the control of a receptor (for IGF-I) in the plasma membrane, and stimulation of the cycle increases nuclear diacylglycerol and apparently induces translocation of protein kinase C to the nucleus. EMBO J 10:3207–3214
22. Duan SZ, Ivashchenko CY, Russell MW, Milstone DS, Mortensen RM (2005) Cardiomyocyte-specific knockout and agonist of peroxisome proliferator-activated receptor-gamma both induce cardiac hypertrophy in mice. Circ Res 97:372–379. doi:10.1161/01.RES.0000179226.34112.6d
23. Eigel BN, Hadley RW (1999) Contribution of the Na(+) channel and Na(+)/H(+) exchanger to the anoxic rise of [Na(+)] in ventricular myocytes. Am J Physiol 277:H1817–H1822
24. Engelhardt S, Hein L, Keller U, Klambt K, Lohse MJ (2002) Inhibition of Na(+)-H(+) exchange prevents hypertrophy, fibrosis, and heart failure in beta(1)-adrenergic receptor transgenic mice. Circ Res 90:814–819. doi:10.1161/01.RES.0000014966.97486.C0
25. Engelhardt S, Hein L, Wiesmann F, Lohse MJ (1999) Progressive hypertrophy and heart failure in beta1-adrenergic receptor transgenic mice. Proc Natl Acad Sci USA 96:7059–7064. doi:10.1073/pnas.96.12.7059
26. Feng Y, Wang Q, Wang Y, Yard B, Lang F (2005) SGK1-mediated fibronectin formation in diabetic nephropathy. Cell Physiol Biochem 16:237–244. doi:10.1159/000089849
27. Firestone GL, Giampaolo JR, O'Keeffe BA (2003) Stimulus-dependent regulation of serum and glucocorticoid inducible protein kinase (SGK) transcription, subcellular localization and enzymatic activity. Cell Physiol Biochem 13:1–12. doi:10.1159/000070244
28. Fliegel L (2009) Regulation of the Na(+)/H(+) exchanger in the healthy and diseased myocardium. Expert Opin Ther Targets 13:55–68. doi:10.1517/14728220802600707
29. Frohlich ED, Gonzalez A, Diez J (2011) Hypertensive left ventricular hypertrophy risk: beyond adaptive cardiomyocytic hypertrophy. J Hypertens 29:17–26. doi:10.1097/HJH.0b013e328340d787
30. Fuster DG, Bobulescu IA, Zhang J, Wade J, Moe OW (2007) Characterization of the regulation of renal Na+/H+ exchanger NHE3 by insulin. Am J Physiol Renal Physiol 292:F577–F585. doi:10.1152/ajprenal.00240.2006
31. Gamper N, Fillon S, Huber SM, Feng Y, Kobayashi T, Cohen P, Lang F (2002) IGF-1 up-regulates K+ channels via PI3-kinase, PDK1 and SGK1. Pflugers Arch 443:625–634. doi:10.1007/s00424-001-0741-5
32. Garciarena CD, Caldiz CI, Correa MV, Schinella GR, Mosca SM, Chiappe de Cingolani GE, Cingolani HE, Ennis IL (2008) Na+/H+ exchanger-1 inhibitors decrease myocardial superoxide production via direct mitochondrial action. J Appl Physiol 105:1706–1713. doi:10.1152/japplphysiol.90616.2008
33. Gehring EM, Zurn A, Klaus F, Laufer J, Sopjani M, Lindner R, Strutz-Seebohm N, Tavare JM, Boehmer C, Palmada M, Lang UE, Seebohm G, Lang F (2009) Regulation of the glutamate transporter EAAT2 by PIKfyve. Cell Physiol Biochem 24:361–368. doi:10.1159/000257428
34. Gilberto DB, Motzel SL, Bone AN, Burns CL, Zeoli AH, Lodge KE, Goode TL (2002) Use of three infusion pumps for postoperative administration of buprenorphine or morphine in dogs. J Am Vet Med Assoc 220:1655–1660, 1650
35. Gonzalez-Robayna IJ, Falender AE, Ochsner S, Firestone GL, Richards JS (2000) Follicle-Stimulating hormone (FSH) stimulates phosphorylation and activation of protein kinase B (PKB/Akt) and serum and glucocorticoid-induced kinase (Sgk): evidence for A kinase-independent signaling by FSH in granulosa cells. Mol Endocrinol 14:1283–1300. doi:10.1210/me.14.8.1283
36. Gruson D, Ginion A, Decroly N, Lause P, Vanoverschelde JL, Ketelslegers JM, Bertrand L, Thissen JP (2011) Urocortin-induced cardiomyocytes hypertrophy is associated with regulation of the GSK-3beta pathway. Heart Vessels. doi:10.1007/s00380-011-0141-5 (in press)
37. Guo D, Kassiri Z, Basu R, Chow FL, Kandalam V, Damilano F, Liang W, Izumo S, Hirsch E, Penninger JM, Backx PH, Oudit GY (2010) Loss of PI3K gamma enhances cAMP-dependent MMP remodeling of the myocardial N-cadherin adhesion complexes and extracellular matrix in response to early biomechanical stress. Circ Res 107:1275–1289. doi:10.1161/CIRCRESAHA.110.229054
38. Hamacher K, Coenen HH, Stocklin G (1986) Efficient stereospecific synthesis of no-carrier-added 2-[18F]-fluoro-2-deoxy-D-glucose using aminopolyether supported nucleophilic substitution. J Nucl Med 27:235–238
39. Haussinger D, Lang F (1991) Cell volume in the regulation of hepatic function: a mechanism for metabolic control. Biochim Biophys Acta 1071:331–350. doi:10.1016/0304-4157(91)90001-D
40. Hoffmann EK, Lambert IH, Pedersen SF (2009) Physiology of cell volume regulation in vertebrates. Physiol Rev 89:193–277. doi:10.1152/physrev.00037.2007
41. Javadov S, Baetz D, Rajapurohitam V, Zeidan A, Kirshenbaum LA, Karmazyn M (2006) Antihypertrophic effect of Na+/H+ exchanger isoform 1 inhibition is mediated by reduced mitogen-activated protein kinase activation secondary to improved mitochondrial integrity and decreased generation of mitochondrial-derived reactive oxygen species. J Pharmacol Exp Ther 317:1036–1043. doi:10.1124/jpet.105.100107
42. Javadov S, Choi A, Rajapurohitam V, Zeidan A, Basnakian AG, Karmazyn M (2008) NHE-1 inhibition-induced cardioprotection against ischaemia/reperfusion is associated with attenuation of the mitochondrial permeability transition. Cardiovasc Res 77:416–424. doi:10.1093/cvr/cvm039

43. Javadov S, Huang C, Kirshenbaum L, Karmazyn M (2005) NHE-1 inhibition improves impaired mitochondrial permeability transition and respiratory function during postinfarction remodelling in the rat. J Mol Cell Cardiol 38:135–143. doi:10.1016/j.yjmcc.2004.10.007
44. Javadov S, Purdham DM, Zeidan A, Karmazyn M (2006) NHE-1 inhibition improves cardiac mitochondrial function through regulation of mitochondrial biogenesis during postinfarction remodeling. Am J Physiol Heart Circ Physiol 291:H1722–H1730. doi:10.1152/ajpheart.00159.2006
45. Javadov S, Rajapurohitam V, Kilic A, Hunter JC, Zeidan A, Said FN, Escobales N, Karmazyn M (2011) Expression of mitochondrial fusion–fission proteins during post-infarction remodeling: the effect of NHE-1 inhibition. Basic Res Cardiol 106:99–109. doi:10.1007/s00395-010-0122-3
46. Javadov S, Rajapurohitam V, Kilic A, Zeidan A, Choi A, Karmazyn M (2009) Anti-hypertrophic effect of NHE-1 inhibition involves GSK-3beta-dependent attenuation of mitochondrial dysfunction. J Mol Cell Cardiol 46:998–1007. doi:10.1016/j.yjmcc.2008.12.023
47. Karmazyn M, Gan XT, Humphreys RA, Yoshida H, Kusumoto K (1999) The myocardial Na(+)-H(+) exchange: structure, regulation, and its role in heart disease. Circ Res 85:777–786
48. Karmazyn M, Kilic A, Javadov S (2008) The role of NHE-1 in myocardial hypertrophy and remodelling. J Mol Cell Cardiol 44:647–653. doi:10.1016/j.yjmcc.2008.01.005
49. Kilic A, Javadov S, Karmazyn M (2009) Estrogen exerts concentration-dependent pro-and anti-hypertrophic effects on adult cultured ventricular myocytes. Role of NHE-1 in estrogen-induced hypertrophy. J Mol Cell Cardiol 46:360–369. doi:10.1016/j.yjmcc.2008.11.018
50. Kobayashi T, Cohen P (1999) Activation of serum- and glucocorticoid-regulated protein kinase by agonists that activate phosphatidylinositide 3-kinase is mediated by 3-phosphoinositide-dependent protein kinase-1 (PDK1) and PDK2. Biochem J 339(Pt 2):319–328. doi:10.1042/0264-6021:3390319
51. Koliakos G, Befani C, Paletas K, Kaloyianni M (2007) Effect of endothelin on sodium/hydrogen exchanger activity of human monocytes and atherosclerosis-related functions. Ann NY Acad Sci 1095:274–291. doi:10.1196/annals.1397.031
52. Kolwicz SC Jr, Tian R (2011) Glucose metabolism and cardiac hypertrophy. Cardiovasc Res 90:194–201. doi:10.1093/cvr/cvr071
53. Kotani K, Yonezawa K, Hara K, Ueda H, Kitamura Y, Sakaue H, Ando A, Chavanieu A, Grigorescu F (1994) Involvement of phosphoinositide 3-kinase in insulin- or IGF-1-induced membrane ruffling. EMBO J 13:2313–2321
54. Lang F, Bohmer C, Palmada M, Seebohm G, Strutz-Seebohm N, Vallon V (2006) (Patho)physiological significance of the serum- and glucocorticoid-inducible kinase isoforms. Physiol Rev 86:1151–1178. doi:10.1152/physrev.00050.2005
55. Lang F, Busch GL, Ritter M, Volkl H, Waldegger S, Gulbins E, Haussinger D (1998) Functional significance of cell volume regulatory mechanisms. Physiol Rev 78:247–306
56. Lang F, Cohen P (2001) Regulation and physiological roles of serum- and glucocorticoid-induced protein kinase isoforms. Sci STKE 2001:re17. doi:10.1126/stke.2001.108.re17
57. Lang F, Gorlach A (2010) Heterocyclic indazole derivatives as SGK1 inhibitors, WO2008138448. Expert Opin Ther Pat 20:129–135. doi:10.1517/13543770903365209
58. Lang F, Klingel K, Wagner CA, Stegen C, Warntges S, Friedrich B, Lanzendorfer M, Melzig J, Moschen I, Steuer S, Waldegger S, Sauter M, Paulmichl M, Gerke V, Risler T, Gamba G, Capasso G, Kandolf R, Hebert SC, Massry SG, Broer S (2000) Deranged transcriptional regulation of cell-volume-sensitive kinase hSGK in diabetic nephropathy. Proc Natl Acad Sci USA 97:8157–8162. doi:10.1073/pnas.97.14.8157
59. Lawrence SP, Holman GD, Koumanov F (2010) Translocation of the Na+/H+ exchanger 1 (NHE1) in cardiomyocyte responses to insulin and energy-status signalling. Biochem J 432:515–523. doi:10.1042/BJ20100717
60. Leineweber K, Aker S, Beilfuss A, Rekasi H, Konietzka I, Martin C, Heusch G, Schulz R (2006) Inhibition of Na+/H+-exchanger with sabiporide attenuates the downregulation and uncoupling of the myocardial beta-adrenoceptor system in failing rabbit hearts. Br J Pharmacol 148:137–146. doi:10.1038/sj.bjp.0706714
61. Leineweber K, Heusch G, Schulz R (2007) Regulation and role of the presynaptic and myocardial Na+/H+ exchanger NHE1: effects on the sympathetic nervous system in heart failure. Cardiovasc Drug Rev 25:123–131. doi:10.1111/j.1527-3466.2007.00010.x
62. Lionetti V, Stanley WC, Recchia FA (2011) Modulating fatty acid oxidation in heart failure. Cardiovasc Res 90:202–209. doi:10.1093/cvr/cvr038
63. Lister K, Autelitano DJ, Jenkins A, Hannan RD, Sheppard KE (2006) Cross talk between corticosteroids and alpha-adrenergic signalling augments cardiomyocyte hypertrophy: a possible role for SGK1. Cardiovasc Res 70:555–565. doi:10.1016/j.cardiores.2006.02.010
64. Morris K (2002) Targeting the myocardial sodium-hydrogen exchange for treatment of heart failure. Expert Opin Ther Targets 6:291–298
65. Mraiche F, Fliegel L (2011) Elevated expression of activated Na(+)/H (+) exchanger protein induces hypertrophy in isolated rat neonatal ventricular cardiomyocytes. Mol Cell Biochem. doi:10.1007/s11010-011-0933-z (in press)
66. Mraiche F, Oka T, Gan XT, Karmazyn M, Fliegel L (2011) Activated NHE1 is required to induce early cardiac hypertrophy in mice. Basic Res Cardiol 106:603–616. doi:10.1007/s00395-011-0161-4
67. Mraiche F, Wagg CS, Lopaschuk GD, Fliegel L (2011) Elevated levels of activated NHE1 protect the myocardium and improve metabolism following ischemia/reperfusion injury. J Mol Cell Cardiol 50:157–164. doi:10.1016/j.yjmcc.2010.10.016
68. Nabeebaccus A, Zhang M, Shah AM (2011) NADPH oxidases and cardiac remodelling. Heart Fail Rev 16:5–12. doi:10.1007/s10741-010-9186-2
69. Naga Prasad SV, Esposito G, Mao L, Koch WJ, Rockman HA (2000) Gbetagamma-dependent phosphoinositide 3-kinase activation in hearts with in vivo pressure overload hypertrophy. J Biol Chem 275:4693–4698. doi:10.1074/jbc.275.7.4693
70. Nakamura TY, Iwata Y, Arai Y, Komamura K, Wakabayashi S (2008) Activation of Na+/H+ exchanger 1 is sufficient to generate Ca2+ signals that induce cardiac hypertrophy and heart failure. Circ Res 103:891–899. doi:10.1161/CIRCRESAHA.108.175141
71. Naray-Fejes-Toth A, Canessa C, Cleaveland ES, Aldrich G, Fejes-Toth G (1999) sgk is an aldosterone-induced kinase in the renal collecting duct. Effects on epithelial Na+ channels. J Biol Chem 274:16973–16978. doi:10.1074/jbc.274.24.16973
72. Nemeth ZH, Deitch EA, Lu Q, Szabo C, Hasko G (2002) NHE blockade inhibits chemokine production and NF-kappaB activation in immunostimulated endothelial cells. Am J Physiol Cell Physiol 283:C396–C403. doi:10.1152/ajpcell.00491.2001
73. Orlowski J, Grinstein S (2004) Diversity of the mammalian sodium/proton exchanger SLC9 gene family. Pflugers Arch 447:549–565. doi:10.1007/s00424-003-1110-3
74. Oudit GY, Penninger JM (2009) Cardiac regulation by phosphoinositide 3-kinases and PTEN. Cardiovasc Res 82:250–260. doi:10.1093/cvr/cvp014

75. Park J, Leong ML, Buse P, Maiyar AC, Firestone GL, Hemmings BA (1999) Serum and glucocorticoid-inducible kinase (SGK) is a target of the PI 3-kinase-stimulated signaling pathway. EMBO J 18:3024–3033. doi:10.1093/emboj/18.11.3024
76. Putney LK, Denker SP, Barber DL (2002) The changing face of the Na+/H+ exchanger, NHE1: structure, regulation, and cellular actions. Annu Rev Pharmacol Toxicol 42:527–552. doi:10.1146/annurev.pharmtox.42.092001.143801
77. Reiter RJ, Manchester LC, Fuentes-Broto L, Tan DX (2010) Cardiac hypertrophy and remodelling: pathophysiological consequences and protective effects of melatonin. J Hypertens 28(Suppl 1):S7–S12. doi:10.1097/01.hjh.0000388488.51083.2b
78. Rexhepaj R, Rotte A, Pasham V, Gu S, Kempe DS, Lang F (2010) PI3 kinase and PDK1 in the regulation of the electrogenic intestinal dipeptide transport. Cell Physiol Biochem 25:715–722. doi:10.1159/000315091
79. Richards JS, Fitzpatrick SL, Clemens JW, Morris JK, Alliston T, Sirois J (1995) Ovarian cell differentiation: a cascade of multiple hormones, cellular signals, and regulated genes. Recent Prog Horm Res 50:223–254
80. Rieder CV, Fliegel L (2003) Transcriptional regulation of Na+/H+ exchanger expression in the intact mouse. Mol Cell Biochem 243:87–95. doi:10.1023/A:1021643608619
81. Rockman HA, Ross RS, Harris AN, Knowlton KU, Steinhelper ME, Field LJ, Ross J Jr, Chien KR (1991) Segregation of atrial-specific and inducible expression of an atrial natriuretic factor transgene in an in vivo murine model of cardiac hypertrophy. Proc Natl Acad Sci USA 88:8277–8281. doi:10.1073/pnas.88.18.8277
82. Rohini A, Agrawal N, Koyani CN, Singh R (2010) Molecular targets and regulators of cardiac hypertrophy. Pharmacol Res 61:269–280. doi:10.1016/j.phrs.2009.11.012
83. Roos A, Boron WF (1981) Intracellular pH. Physiol Rev 61:296–434
84. Rotte A, Bhandaru M, Foller M, Biswas R, Mack AF, Friedrich B, Rexhepaj R, Nasir O, Ackermann TF, Boini KM, Kunzelmann K, Behrens J, Lang F (2009) APC sensitive gastric acid secretion. Cell Physiol Biochem 23:133–142
85. Rotte A, Mack AF, Bhandaru M, Kempe DS, Beier N, Scholz W, Dicks E, Potzsch S, Kuhl D, Lang F (2009) Pioglitazone induced gastric acid secretion. Cell Physiol Biochem 24:193–200
86. Rotte A, Pasham V, Yang W, Eichenmuller M, Bhandaru M, Shumilina E, Lang F (2010) Phosphoinositide 3-kinase-dependent regulation of Na+/H+ exchanger in dendritic cells. Pflugers Arch 460:1087–1096
87. Sarigianni M, Tsapas A, Mikhailidis DP, Kaloyianni M, Koliakos G, Paletas K (2010) Involvement of signaling molecules on Na/H exchanger-1 activity in human monocytes. Open Cardiovasc Med J 4:181–188
88. Segalen C, Longnus SL, Baetz D, Counillon L, Van Obberghen E (2008) 5-Aminoimidazole-4-carboxamide-1-beta-D-ribofuranoside reduces glucose uptake via the inhibition of Na+/H+ exchanger 1 in isolated rat ventricular cardiomyocytes. Endocrinology 149:1490–1498. doi:10.1210/en.2007-1326
89. Shigaev A, Asher C, Latter H, Garty H, Reuveny E (2000) Regulation of sgk by aldosterone and its effects on the epithelial Na(+) channel. Am J Physiol Renal Physiol 278:F613–F619
90. Snabaitis AK, Cuello F, Avkiran M (2008) Protein kinase B/Akt phosphorylates and inhibits the cardiac Na+/H+ exchanger NHE1. Circ Res 103:881–890. doi:10.1161/CIRCRESAHA.108.175877
91. Steffan JJ, Williams BC, Welbourne T, Cardelli JA (2010) HGF-induced invasion by prostate tumor cells requires anterograde lysosome trafficking and activity of Na+-H+ exchangers. J Cell Sci 123:1151–1159. doi:10.1242/jcs.063644
92. Vallon V, Wyatt AW, Klingel K, Huang DY, Hussain A, Berchtold S, Friedrich B, Grahammer F, Belaiba RS, Gorlach A, Wulff P, Daut J, Dalton ND, Ross J Jr, Flogel U, Schrader J, Osswald H, Kandolf R, Kuhl D, Lang F (2006) SGK1-dependent cardiac CTGF formation and fibrosis following DOCA treatment. J Mol Med 84:396–404. doi:10.1007/s00109-005-0027-z
93. Voelkl JG, Haubner BJ, Kremser C, Mayr A, Klug G, Loizides A, Muller S, Pachinger O, Schocke M, Metzler B (2011) Cardiac imaging using clinical 1.5 T MRI scanners in a murine ischemia/reperfusion model. J Biomed Biotechnol 2011:185683. doi:10.1155/2011/185683
94. Waisbren SJ, Geibel J, Boron WF, Modlin IM (1994) Luminal perfusion of isolated gastric glands. Am J Physiol 266:C1013–C1027
95. Waldegger S, Barth P, Raber G, Lang F (1997) Cloning and characterization of a putative human serine/threonine protein kinase transcriptionally modified during anisotonic and isotonic alterations of cell volume. Proc Natl Acad Sci USA 94:4440–4445. doi:10.1073/pnas.94.9.4440
96. Waldegger S, Klingel K, Barth P, Sauter M, Rfer ML, Kandolf R, Lang F (1999) h-sgk serine-threonine protein kinase gene as transcriptional target of transforming growth factor beta in human intestine. Gastroenterology 116:1081–1088. doi:10.1016/S0016-5085(99)70011-9
97. Wang D, Zhang H, Lang F, Yun CC (2007) Acute activation of NHE3 by dexamethasone correlates with activation of SGK1 and requires a functional glucocorticoid receptor. Am J Physiol Cell Physiol 292:C396–C404. doi:10.1152/ajpcell.00345.2006
98. Wang Y, Meyer JW, Ashraf M, Shull GE (2003) Mice with a null mutation in the NHE1 Na+-H+ exchanger are resistant to cardiac ischemia-reperfusion injury. Circ Res 93:776–782. doi:10.1161/01.RES.0000094746.24774.DC
99. Wulff P, Vallon V, Huang DY, Volkl H, Yu F, Richter K, Jansen M, Schlunz M, Klingel K, Loffing J, Kauselmann G, Bosl MR, Lang F, Kuhl D (2002) Impaired renal Na(+) retention in the sgk1-knockout mouse. J Clin Invest 110:1263–1268. doi:10.1172/JCI200215696
100. Xue J, Mraiche F, Zhou D, Karmazyn M, Oka T, Fliegel L, Haddad GG (2010) Elevated myocardial Na+/H+ exchanger isoform 1 activity elicits gene expression that leads to cardiac hypertrophy. Physiol Genomics 42:374–383. doi:10.1152/physiolgenomics.00064.2010
101. Yokoyama H, Gunasegaram S, Harding SE, Avkiran M (2000) Sarcolemmal Na+/H+ exchanger activity and expression in human ventricular myocardium. J Am Coll Cardiol 36:534–540. doi:10.1016/S0735-1097(00)00730-0
102. Yu W, Chen C, Fu Y, Wang X, Wang W (2010) Insulin signaling: a possible pathogenesis of cardiac hypertrophy. Cardiovasc Ther 28:101–105. doi:10.1111/j.1755-5922.2009.00120.x
103. Yun CC, Chen Y, Lang F (2002) Glucocorticoid activation of Na(+)/H(+) exchanger isoform 3 revisited. The roles of SGK1 and NHERF2. J Biol Chem 277:7676–7683. doi:10.1074/jbc.M107768200